VALENTE, E. J., SANTARSIERO, B. D. & SCHOMAKER, V. (1979). *J. Org. Chem.* **44**, 798–802.
VALENTE, E. J. & TRAGER, W. F. (1978). *J. Med. Chem.* **21**, 141–143.
VALENTE, E. J., TRAGER, W. F. & JENSEN, L. H. (1975). *Acta Cryst.* B**31**, 954–960.
WEST, B. D., PREIS, S., SCHROEDER, C. & LINK, K. P. (1961). *J. Am. Chem. Soc.* **83**, 2676–2679.

Acta Cryst. (1990). B**46**, 637–643

Low-Resolution Models for Ribosomal Particles Reconstructed from Electron Micrographs of Tilted Two-Dimensional Sheets

BY Z. BERKOVITCH-YELLIN

Department of Structural Chemistry, Weizmann Institute of Science, Rehovot, Israel, and Max-Planck-Institute for Molecular Genetics, D-1000 Berlin 33, Federal Republic of Germany

H. G. WITTMANN

Max-Planck-Institute for Molecular Genetics, D-1000 Berlin 33, Federal Republic of Germany

AND A. YONATH

Department of Structural Chemistry, Weizmann Institute of Science, Rehovot, Israel, and Max-Planck-Research Unit for Structural Molecular Biology, D-2000 Hamburg 52, Federal Republic of Germany

(*Received* 17 *July* 1989; *accepted* 20 *March* 1990)

Abstract

Models of the whole ribosome (70S) and its large subunit (50S) were obtained at low resolution (47 and 28 Å respectively) by three-dimensional image reconstruction using diffraction data collected from electron micrographs of two-dimensional ordered arrays. The comparison of the various reconstructed images, using interactive computer graphics, enabled the assessment of the reliability of the method, the derivation of the shape of the small subunit (30S) and the assignment of several functional features such as the probable path taken by the nascent protein chain, the presumed site for the process of biosynthesis of proteins, and a feasible mode for tRNA binding. The reconstructed models of the various ribosomal particles may be used for phasing of X-ray diffraction data at low resolution.

Introduction

Structural information is essential for a detailed understanding of the mechanisms of biological processes. The biosynthesis of proteins requires several enzymatic and recognition processes which take place on the ribosomes, the cell organelles where the genetic information is translated into polypeptide chains. The ribosomes are built of two subunits of unequal size which associate upon initiation of protein synthesis. The molecular weights of bacterial ribosomes and their large and small subunits are $2{\cdot}3 \times 10^6$, $1{\cdot}45 \times 10^6$ and $8{\cdot}5 \times 10^5$ daltons and their sedimentation coefficients 70S, 50S and 30S, respectively. The ribosomes are complex assemblies with no internal symmetry, composed of several strands of RNA and a large number of different proteins. A typical large subunit of ribosomes from bacterial sources contains 34–36 different proteins and two RNA chains; the small one is composed of 21 proteins and one RNA chain.

The large size of ribosomal particles, which is an obstacle for crystallographic studies, permits their investigation by electron microscopy. In fact these two techniques may complement each other in structural studies on assemblies with the size of ribosomes: electron microscopy, combined with image reconstruction using Fourier methods, should lead to the determination of the overall shape of the whole ribosome as well as its subunits. These, in turn, may serve as starting models for rotation and translation searches, using X-ray data, aimed at the establishment of the location and orientation of the particles within their respective crystal lattice, information which is most valuable for extracting initial phases at low resolution.

The images of 70S and 50S ribosomal particles from *B. stearothermophiles* were reconstructed at 47 and 28 Å resolution respectively, using data obtained from the diffraction patterns of electron micrographs from two or more tilt series of two-dimensional

0108-7681/90/050637-07$03.00

sheets (Yonath, Leonard & Wittmann, 1987; Arad, Piefke, Weinstein, Gewitz, Yonath & Wittmann, 1987; Yonath & Wittmann, 1989). In both cases the particles are packed as dimers in relatively small unit cells (192×420 and 152×350 Å respectively). Several features have been clearly observed by us and by others in the reconstructed images (Milligan & Unwin, 1986; Wagenknecht, Carazo, Radamacher & Frank, 1989). Among them is a tunnel of length 100–120 Å and diameter of up to 25 Å, which spans the large subunit (Fig. 1) and an empty space in the 70S ribosome, which occupies 15–20% of the total volume (Fig. 2*a*).

A thorough examination and comparison of the reconstructed images of the ribosome and its large subunit, with the aid of interactive computer graphics, yielded a tentative assignment of the two ribosomal subunits on the whole (70S) ribosome, as well as several functional features such as the path taken by the nascent protein chain (Yonath *et al.*, 1987), the site where the actual process of protein biosynthesis takes place (Arad, Piefke, Weinstein *et al.*, 1987), and the site for codon–anticodon interaction. Based on these observations we were able to suggest a possible mode for tRNA binding (Yonath & Wittmann, 1989). In this paper we describe our interpretation of the reconstructed models, and their use for the derivation of low-resolution phases of X-ray data collected from crystals of the respective ribosomal particles.

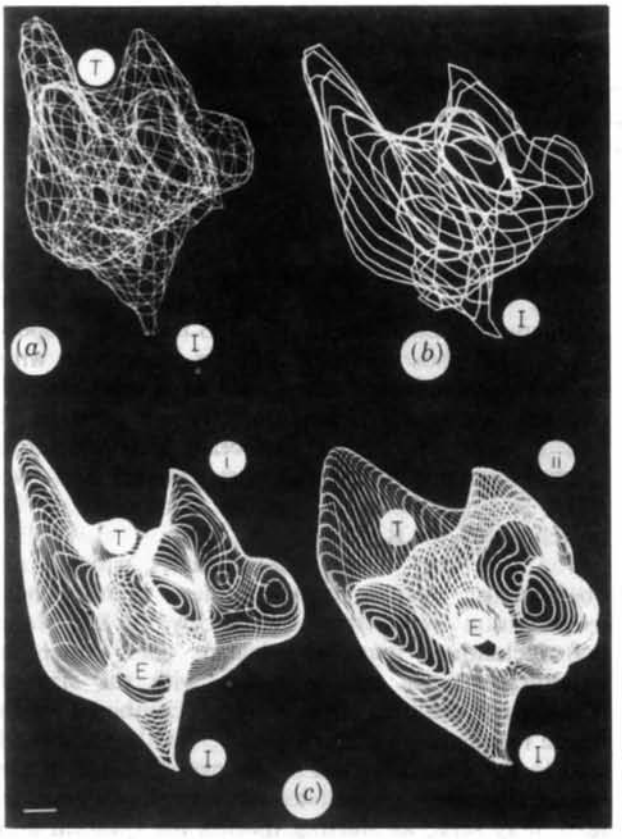

Fig. 1. A display of the outline of the reconstructed model of the 50S ribosomal subunit at 30 Å resolution. Several views are shown. Bar length = 20 Å. (I) marks the contact between two particles in the crystal. (T) is at the cleft between the projecting arms, at the site where it turns into the tunnel. (E) marks the exit of the tunnel. (*a*) The 50S particles are displayed as a net which is a contour map of the outer envelope of the particle. In (*b*) and (*c*) 50S subunit is displayed as a 'molecule'. The two-dimensional density sections which were used for the derivation of the 'atomic' coordinates of these 'molecules' are parallel to the two-dimensional sheet plane with grid steps of size 10 Å in (*b*) and 5 Å in (*c*).

Experimental

The procedures used for the preparation of the ribosomal particles, for the growth of the two-dimensional sheets as well as for the image-reconstruction studies were described by Piefke *et al.* (1986), Yonath *et al.* (1987), Arad, Piefke, Weinstein *et al.* (1987) and Arad, Piefke, Gewitz *et al.* (1987). The electron density maps were computed from the diffraction data using the program *GHC*650 (G. H. Cohen, National Institute of Health, modified by J. L. Sussmann, Weizmann Institute), the program *FRODOMAP* (T. N. Bhat, National Institute of Health) as well as the *EMBL* version (written by H. Bosshard). For real-time display of the reconstructed images, drawn as contour maps, we used the computer program *FRODO* (Jones, 1978) in its version specifically designed for the Evans and Sutherland PS300 graphics system (Pflugrath, Saper & Quicho, 1984). To enable the use of *FRODO* for the display of structures as large as those of ribosomes, with unit-cell dimensions of a few hundred ångstroms, we divided the cell dimensions by ten and treated all the distances as being ten times smaller. In *FRODO* a density map in the background can be compared with atoms or molecules which are shown either in the foreground or background of the display. To allow comparison of two (or more) density maps we have written a routine which enabled definition of a density contour map as a macromolecule composed of 'atoms' situated along the various contour lines, and thus enabled its display and manipulation in a similar fashion to that of molecules in the original *FRODO* program. For the comparison of two (or more) density maps we used *FRODO*'s function *FBRT* which is commonly used to move (rotate or translate) a group of connected atoms.

Results and discussion

Our reconstructed images are displayed as contour maps similar to electron density maps. For our

models, derived from negatively stained two-dimensional sheets, these show regions of stain rejection. It is noteworthy that the models obtained by three-dimensional image reconstruction of electron microscope data may suffer from shrinkage of the specimens caused by the preparative treatment for electron microscopy. To compensate for such shrinkage we slightly expanded the density maps of the ribosome and its subunit. To find the appropriate degree for the expansion we compared the unit-cell dimensions of the 70S ribosome with the corresponding vectors in the cell of the large (50S) subunit. We found that a reasonable fit between these two is obtained when the density of the 70S particle is expanded by 10% along the *a* axis and that of the 50S particle by 8% along the *b* axis of each respective unit cell. These values are still lower than those commonly observed in electron microscopy, hence it is conceivable that these corrections do not take account of the entire shrinkage (which may reach a value of 25%). Another cause for a possible deformation of the reconstructed images is the limitation in the tilt angles (which cannot exceed 60°), which leads to a large 'missing cone' in the direction perpendicular to the tilt axis. These factors may result in some uncertainty in the dimension of the reconstructed particles along the perpendicular direction.

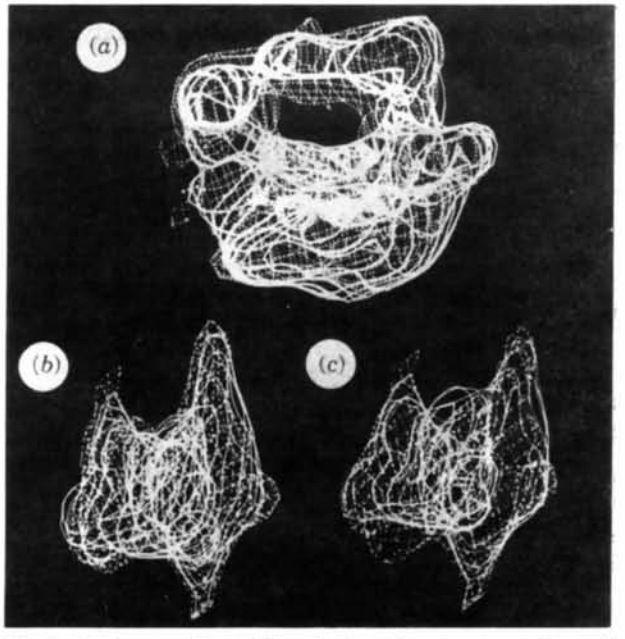

Fig. 2. (*a*) Superposition of two independent reconstructions of the 70S ribosome at 50 Å resolution. (*b*) Superposition of two 50S particles reconstructed at 30 Å resolution. (*c*) The 50S subunit as reconstructed at 30 Å (net) and 50 Å resolution (lines). One image is shown in full lines and the other in dotted ones.

The possibility of representing the reconstructed particles as 'atoms' or 'molecules' (in the *FRODO* terminology) facilitated a visual comparison between differently reconstructed particles. This enabled estimation of the reliability and reproducibility of the results obtained by image reconstruction in general and of our results in particular.

We compared the details of the shape of two slightly different images obtained in the reconstruction of the 70S ribosome (Fig. 2*a*), and of the 50S subunit (Fig. 2*b*), as well as the reconstructed images for the latter obtained at two different resolutions (28 and 47 Å) (Fig. 2*c*). We found that although there were variations in the details and the quality of different reconstructions, for both the 70S and 50S particles, the overall features of the respective particles are similar. Moreover, within the experimental errors (mainly shrinkage), the dimensions of all the reconstructed images are similar to those determined by other physical methods (Wittmann, 1983; Hardesty & Kramer, 1986).

We next compared the shapes of the whole ribosome and its large subunit (Fig. 3). The image of the 50S particle was fitted into that of the 70S at two different resolutions, 50 and 30 Å, to account for the difference in resolution at which the two particles were reconstructed. The comparison was performed on the graphics system taking advantage of similar features of the fitted images, in particular the tunnel of 25 Å diameter and 100 Å length, which was observed in both. We found that there is a structural similarity between the part associated with the 50S subunit within the whole ribosome and the unbound particle, and that even at 50 Å resolution most of the common features of the large subunit and the whole ribosome are resolved (Fig. 3*a*). The overall agreement in the reconstructed shape of the isolated and bound 50S particles is rather striking. However, there are two regions in which the densities of the two models differ slightly (Fig. 3*a*). At this stage it is not clear whether these differences reflect conformational changes occurring upon association of the subunits, or are a consequence of the low resolution of the reconstructions.

It is noteworthy that we have also tried to fit the density maps of the 50S and 70S subunits using the density-correlation program of Bricogne (1976) and *ULTIMA* (Rabinovich & Shakked, 1984). The density of the large subunit (50S) was treated as the model input molecule (in the latter) and the envelope (in the former). We tried to find regions in 70S density map which will best correlate with that of the 50S. So far these efforts have not yielded fits comparable in quality to that obtained by the visual matching on the graphics screen.

After fitting the density of the large subunit into that of the whole ribosome we computed a difference

map (Fig. 3*b*) by eliminating from the density of the 70S subunit those parts which were correlated with the density of the large subunit. From this residual map we derived a model for the shape of the small subunit (30S) (Fig. 4). So far, the image of this particle has not been independently reconstructed since two-dimensional sheets of the small subunit, suitable for three-dimensional image reconstruction studies, are not yet available. There is a similarity in the shape of the small subunit (30S) obtained in this way and that observed by visualization of single particles (Wittmann, 1983). However, isolated 30S particles appear in the electron microscope somewhat wider than the reconstructed ones. This may be due either to the different conformation of associated particles or to flattening of the isolated particles which occurs as a result of their contact with the microscope grids.

Staining of the two-dimensional arrays of the 70S ribosomes with uranyl acetate led to the observation of regions where uranyl acetate, acting as a positive stain, was incorporated into the particles. This may indicate that in these regions the RNA, the natural candidate for interacting with this stain, is concentrated and exposed to the stain. Examples of such regions are the edges at the interface of the small and the large subunit, in agreement with previous studies (Milligan & Unwin, 1986). Another RNA-rich region was found on that part of the ribosome which was assigned as 30S (Arad, Piefke, Weinstein *et al.*, 1987). This region contains a groove which was clearly seen in the reconstructed model (Fig. 2). Based on biochemical and other structural studies (Hardesty & Kramer, 1986; Brimacombe, Atmadja, Stiege & Schuler, 1988) we have assigned this region as the 'neck' which is the location of mRNA and tRNA binding. This groove is located at a distance of about 70 Å from the entrance to the tunnel.

There is a substantial discrepancy between the ability of ribosomes to bind tRNA and the efficiency of protein biosynthesis. Thus, in the presence of 10–15 n*M* Mg^{2+} poly(U)-programmed 70S ribosomes are 80–100% active in binding peptidyl tRNA

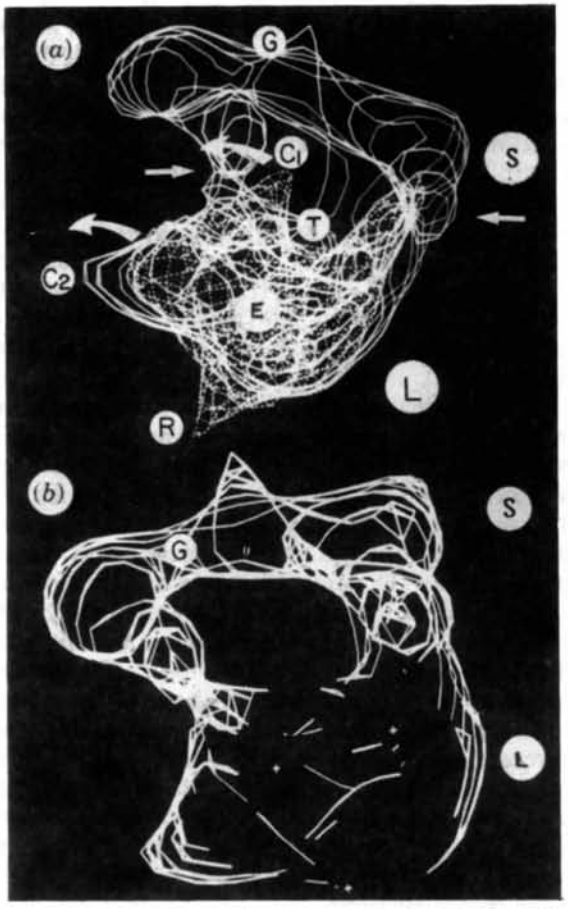

Fig. 3. (*a*) Superposition of computer-graphics displays of the outline of the reconstructed models of the 70S ribosome (in lines) and of the 50S ribosomal subunit (dotted net). (*b*) A difference density map computed after fitting the densities of the 70S and the large subunits. (S) and (L) indicate the small (30S) and the large (50S) subunits, respectively. The arrows point to the interface between the two subunits. (G) marks the groove rich in RNA in the small subunit. (T) shows the cleft and the entrance to the tunnel and (E) shows the exit site. The extra density (R) is a consequence of the different resolutions at which the two models were reconstructed (30 and 47 Å). (C1) and (C2) indicate regions of extra density in the models of the 50S subunit and the 70S ribosome, respectively. These may be a result of conformational changes upon association. The curved arrows indicate possible directions for cooperative movement at these regions.

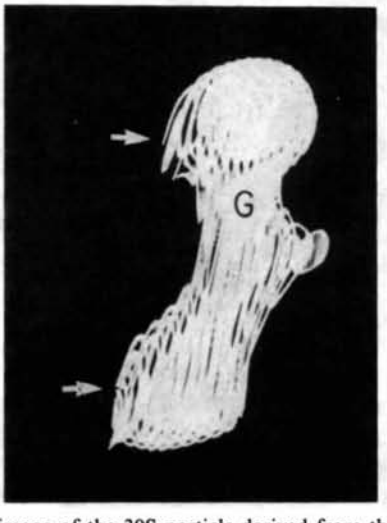

Fig. 4. The image of the 30S particle derived from the difference map. The density maps which were used for the derivation of this particle were computed over a fine grid (see caption to Fig. 1*c*). The two arrows indicate the contacts with the large subunit. (G) is at the groove where the mRNA may bind to the ribosome.

analogues, but only a fraction (approximately 60%) of such ribosomes primed with AcPhe-tRNA participate in poly(U)-directed poly(Phe) synthesis. Recently, it was found (Rheinberger & Nierhaus, 1990) that the majority of the apparently 'inactive' ribosomes are actually able to participate in peptide bond formation, but lose their activity at the stage of the formation of di- or tripeptides. It seems, therefore, that the first two rounds of elongation are a critical step in protein biosynthesis. A possible explanation is that the elongation of the nascent protein takes place only if the newly formed peptide is properly fixed in the presumed excretion tunnel.

It has been established (Rheinberger & Nierhaus, 1983) that there are three distinct sites for binding tRNA on the ribosome. During the biosynthetic process at least two sites are occupied on the ribosome. Furthermore, *in vitro* one can even find conditions for simultaneous binding of three tRNA molecules. In the light of these observations we tried to fit a molecule of tRNA (Sussman, Holbrook, Warrant, Church & Kim, 1978) in the empty space within the 70S particle, so that its anticodon end is near the presumed site of mRNA binding and the CCA end at the protein biosynthesis site. As seen in Fig. 5(*a*), a molecule of tRNA can easily bridge between the presumed coding region (on the groove on the 30S subunit) and the peptidyl transferase center (on the 50S subunit). In fact, the void is large enough to accommodate one or even two more tRNA molecules (Figs. 5*b* and 5*c*) and several additional components (*e.g.* elongation factors) which take part in protein biosynthesis.

A detailed assignment of the functional domains of the ribosome, studied by other methods, to the various structural features of our model still awaits further investigations. In view of the recent progress of our crystallographic studies and of our ability to reproducibly obtain two-dimensional sheets of native, as well as modified ribosomal particles, we hope that we shall be able to locate specific sites on a detailed model in the forseeable future.

In an attempt to exploit the reconstructed models for initial phasing of X-ray data collected for the whole ribosome and its subunits, we generated various possible packing arrangements of the ribosomal particles in their respective crystal lattices (Figs. 6, 7). The idea was to recognize some patterns observed by electron microscopy of positively stained sections of embedded three-dimensional crystals of the various ribosomal particles (Glotz *et al.*, 1987; Trakhanov *et al.*, 1987). Computer graphics, with the program *FRODO*, was also found to be useful for these exercises owing to the relative ease of the display of crystal structures once space group, unit-cell dimensions, symmetry and the contents of one asymmetric unit are known (or assumed).

The small ribosomal subunit packs in a crystal of space group $P42_12$ with unit-cell dimensions $a = b = 407$ and $c = 172$ Å. There are two molecules in the asymmetric unit (Yonath *et al.*, 1988). The approxi-

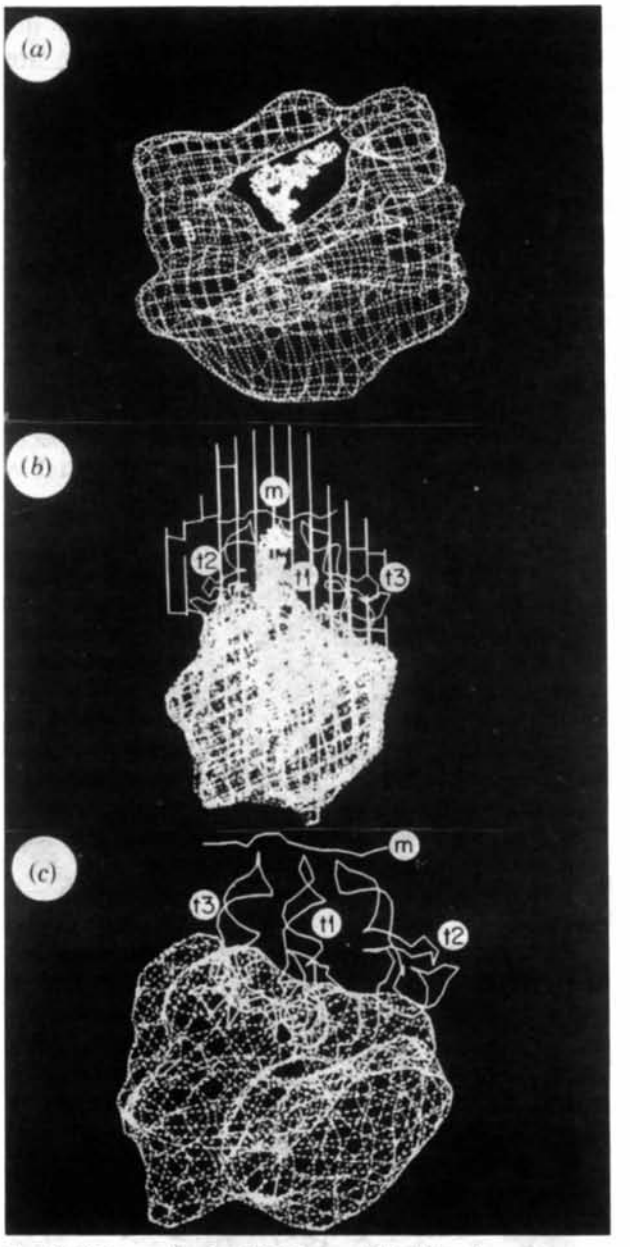

Fig. 5. (*a*) One molecule of tRNA 'model-built' in the empty space observed in a 70S particle. (*b*) Three molecules of tRNA (t1,t2,t3) with a section of 28 ribonucleotides (in an arbitrary conformation), which may simulate the mRNA (m) fitted in the empty space at the 70S, side view. The 70S particle is shown as parallel lines. The tRNA molecule which points directly into the tunnel is highlighted (by including all the atoms). (*c*) The 50S particle with a section of 28 nucleotides which may simulate the mRNA (m) and the three tRNA molecules as in (*b*). The 70S particle was removed for clarity and only the outlines of the tRNA molecules are shown.

mate dimensions of the reconstructed 30S particle are $190 \times 90 \times 90$ Å^3 (Fig. 4). Because of the similarity between the dimensions of the particle and those of its crystal unit-cell vectors, (*i.e.* 190 Å is similar to the length of the *c* axis and to half of the *a* and the *b* axes), we considered two distinctly different orientations which the particles may adopt in the lattice. According to the first, the 30S particles are roughly aligned with their long molecular axis along the crystal *a* and *b* axes forming *ab* layers. Adjacent layers are composed of two different 30S particles, which are the pair of molecules in the asymmetric unit. In a second distinctly different motif, the 30S particles are oriented with their long molecular axis along the crystal *c* axis which is of a similar length. We have generated various speculative packing arrangements, which differ from each other by the orientation of the molecules in the asymmetric unit, as well as that of the pair in the unit cell (Fig. 6). The arrangements are different from one another, but all are characterized by having a substantial 'free' space. This indicates that a large portion of the crystal is filled with solvent, in agreement with the results obtained by electron microscopy of embedded crystals (Glotz *et al.*, 1987).

In generating various speculative packing arrangements for the crystal of the 50S subunit of *Halobacterium marismortui* we took advantage of the similarities between two space-group symmetries which were assigned for these particles, *i.e.* $C222_1$ with $a = 215$, $b = 300$ and $c = 590$ Å with one particle in the asymmetric unit (Yonath & Wittmann, 1989) and $P2_1$ with $a = 182$, $b = 584$, $c = 186$ Å, $\beta = 109°$ (Makowski, Frolow, Saper, Shoham, Wittmann & Yonath, 1987).

We will next employ the reconstructed images of the ribosomal particles, represented as pseudo molecules, as models in rotation and translation searches using X-ray data collected from crystals of the various particles (Yonath *et al.*, 1988; Yonath & Wittmann, 1989; Makowski *et al.*, 1987; Berkovitch-Yellin *et al.*, 1990), using the computer programs *MERLOT* (Fitzgerald, 1988) and *ULTIMA*

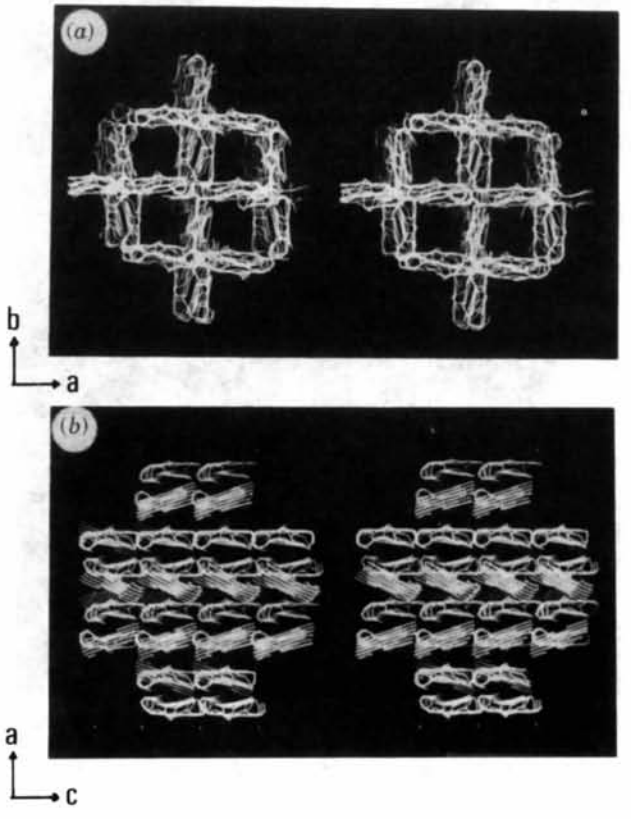

Fig. 6. Speculative packing arrangements of ribosomal particles: (*a*) and (*b*) are stereopairs of two possible distinctly different packing arrangements for the 30S particles. Lattice points are marked by dots. Owing to the limitation of the dimensions of the display program only a rough outline of the particles is shown.

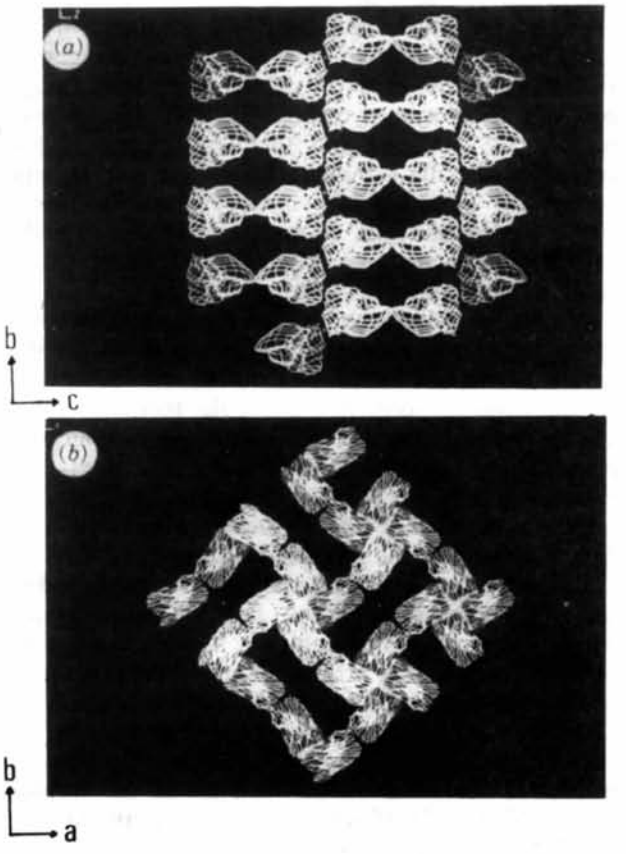

Fig. 7. Speculative packing arrangements of ribosomal particles (D. Rabinovich, unpublished): (*a*) 50S particles, in space group $C222_1$, (*b*) 70S particles, in space group $P4_12_12$. Lattice points are marked by dots. Owing to the limitation of the dimensions of the display program only a rough outline of the particles is shown.

(Rabinovich & Shakked, 1984). Initially, only very low-order reflections (less than 40 Å resolution) will be used for the searches.

We would like to thank Drs K. Nierhaus and H. J. Rheinberger for very stimulating discussions, J. Piefke and T. Arad for their outstanding contribution to this work in conducting the electron microscopy experiments, Professor D. Rabinovich for his constant interest and help, Professor J. L. Sussman for his enthusiasm and willingness to adapt the computer display programs, Dr K. R. Leonard for his active interest and critical comments, Drs B. Shaanan, H. Bosshard, M. A. Saper and Mr A. Levy for assistance with computer problems, as well as H. S. Gewitz, J. Müssig, C. Glotz, B. Romberg and J. Halfon for skillful technical assistance.

This work was supported by research grants from BMFT(MPBO 180), NIH (GM 34360), Heineman (4694 81) and the Kimmelman Center for Biomolecular Structure and Assembly. ZBY is a Minerva fellow and AY holds the Martin Kimmel professorial chair.

References

ARAD, T., PIEFKE, J., GEWITZ, H. S., HENNEMANN, B., GLOTZ, C., MUSSIG, J., YONATH, A. & WITTMANN, H. G. (1987). *Anal. Biochem.* **167**, 113–117.

ARAD, T., PIEFKE, J., WEINSTEIN, S., GEWITZ, H. S., YONATH, A. & WITTMANN, H. G. (1987). *Biochimie*, **69**, 1001–1006.

BERKOVITCH-YELLIN, Z., HANSEN, H. A. S., BENNETT, W. S., SHARON, R., VON BOEHLEN, K., VOLKMANN, N., PIEFKE, J., YONATH, A. & WITTMANN, H. G. (1990). *J. Cryst. Growth*. In the press.

BRICOGNE, G. (1976). *Acta Cryst.* A**32**, 832–846.

BRIMACOMBE, R., ATMADJA, J., STIEGE, W. & SCHULER, D. (1988). *J. Mol. Biol.* **199**, 115–136.

FITZGERALD, P. M. (1988). *J. Appl. Cryst.* **21**, 273–278.

GLOTZ, C., MUSSIG, J., GEWITZ, H. S., MAKOWSKI, I., ARAD, T., YONATH, A. & WITTMANN, H. G. (1987). *Biochem. Int.* **15**, 953–960.

HARDESTY, B. & KRAMER, G. (1986). Editors. *Structure, Function and Genetics of Ribosomes*. Heidelberg, New York: Springer-Verlag.

JONES, T. A. (1978). *J. Appl. Cryst.* **11**, 268–272.

MAKOWSKI, I., FROLOW, F., SAPER, M. A., SHOHAM, M., WITTMANN, H. G. & YONATH, A. (1987). *J. Mol. Biol.* **193**, 819–822.

MILLIGAN, R. A. & UNWIN, P. N. T. (1986). *Nature (London)*, **319**, 693–695.

PFLUGRATH, J. W., SAPER, M. A. & QUICHO, F. A. (1984). *Methods and Applications in Crystallographic Computing*, edited by S. HALL & T. ASHIAKA, p. 407. Oxford: Clarendon Press.

PIEFKE, J., ARAD, T., MAKOWSKI, I., GEWITZ, H. S., HENNEMAN, B., YONATH, A. & WITTMANN, H. G. (1986). *FEBS Lett.* **209**, 104–106.

RABINOVICH, D. & SHAKKED, Z. (1984). *Acta Cryst.* A**40**, 195–200.

RHEINBERGER, H.-J. & NIERHAUS, K. H. (1983). *Proc. Natl Acad. Sci. USA*, **80**, 4213–4217.

RHEINBERGER, H.-J. & NIERHAUS, K. H. (1990). Submitted.

SUSSMAN, J. L., HOLBROOK, S. R., WARRANT, R. W., CHURCH, G. M. & KIM, S.-H. (1978). *J. Mol. Biol.* **123**, 607–630.

TRAKHANOV, S. D., YUSUPOV, M. M., AGALAROV, S. C., GARBER, M. B., RYAZANTSEV, S. N., TISCHENKO, S. V. & SHIROKOV, V. A. (1987). *FEBS Lett.* **220**, 319–322.

WAGENKNECHT, T., CARAZO, J. M., RADAMACHER, M. & FRANK, J. (1989). *Biophys. J.* **55**, 455–464.

WITTMANN, H. G. (1983). *Annu. Rev. Biochem.* **52**, 35–65.

YONATH, A., GLOTZ, C., GEWITZ, H. S., BARTELS, K. S., VON BOHLEN, K., MAKOWSKI, I. & WITTMANN, H. G. (1988). *J. Mol. Biol.* **203**, 831–834.

YONATH, A., LEONARD, K. R. & WITTMANN, H. G. (1987). *Science*, **236**, 813–816.

YONATH, A. & WITTMANN, H. G. (1989). *Trends Biochem. Sci.* **14**, 329–335.

Acta Cryst. (1990). B**46**, 643–645

Thermal Motion Analysis in [5]-, [6]- and [7]-Circulene Crystals: a Harmonic Lattice-Dynamical Calculation

BY GIUSEPPE FILIPPINI

Centro del CNR c/o Dipartimento di Chimica Fisica ed Elettrochimica, Università di Milano, via Golgi 19, *I*-20133 *Milano, Italy*

(*Received* 6 *December* 1989; *accepted* 28 *March* 1990)

Abstract

A harmonic lattice-dynamical model has been used to calculate crystallographic atomic displacement parameters (a.d.p.'s) for crystals of [5]-circulene (corannulene) at 293 and 203 K, [6]-circulene (coronene) and [7]-circulene at 293 and 163 K. Empirical internal and external force fields, which were derived for a series of other aromatic hydrocarbons, have been employed. The agreement between calculated and experimental a.d.p.'s is very good: this is particularly promising in view of the extension

0108-7681/90/050643-03$03.00